On-ground performance tests of the SAX/PDS detector (*)

F. FRONTERA[1][2], M. N. CINTI[1], D. DAL FIUME[1], G. LANDINI[1]
L. NICASTRO[1], M. ORLANDINI[1], G. ZAVATTINI[2], E. COSTA[3]
R. S. SCHREINER[4], C. M. ROSZA[4], P. S. RABY[4], J. WHITE[4]
V. CHIAVERINI[5], F. MONZANI[5], J. M. POULSEN[5] and E. SUETTA[6]

[1] *Istituto Tecnologie e Studio Radiazioni Extraterrestri, CNR - Bologna, Italy*
[2] *Dipartimento di Fisica, Università di Ferrara - Ferrara, Italy*
[3] *Istituto di Astrofisica Spaziale, CNR - Frascati,Italy*
[4] *Bicron Corporation - New Bury, OH, USA*
[5] *LABEN SpA - Vimodrone, Milano, Italy*
[6] *Officine Galileo - Campi Bisenzio, Firenze, Italy*

Summary. — The Phoswich Detection System (PDS) is one of the four narrow field experiments on board the SAX satellite. The PDS will be dedicated to deep temporal and spectral studies of celestial X-ray sources in the 15–300 keV energy band. It also includes a gamma-ray burst monitor. The PDS detector is composed of 4 actively shielded NaI(Tl)/CsI(Na) phoswich scintillators with a total geometric area of 795 cm^2 and a field of view of $1.4°$ (FWHM). The performance of the detector, before its integration with its flight electronic, was tested using standard instrumentation. Here we present results of these tests. The measured energy resolution of the phoswich units is better than 15% at 60 keV, confirming the expectations. Also test results of the antico-incidence shield of CsI(Na) and collimator are discussed.

PACS 96.40 – Cosmic rays.
PACS 98.70.Qy – X-ray sources.
PACS 01.30.Cc – Conference proceedings.

1. – Introduction

The three-axis–stabilized satellite for X-ray astronomy SAX is a joint program of the Italian Space Agency (ASI) and the Netherlands Agency for Aerospace Programs (NIVR). SAX was launched in April 1996 into a circular orbit at 600 km altitude with $4.2°$ inclination. An overview of the SAX mission can be found elsewhere [1]. The payload includes Narrow-Field Instruments (NFIs) and Wide-Field Cameras (WFCs). The NFIs

are four Concentrators Spectrometers (C/S) with 3 units operating in the 1–10 keV energy band and 1 unit operating in 0.1–10 keV, a High Pressure Gas Scintillation Proportional Counter (HPGSPC) operating in the 3–120 keV energy band and a Phoswich Detection System (PDS) with four detection units operating in the 15–300 keV energy band. Orthogonally with respect to the NFIs there are two WFCs (field of view of $20° \times 20°$ FWHM) which operate in the 2–30 keV energy band.

Descriptions of the PDS design have already been reported [2, 3]. In this paper we report results of on-ground tests devoted to investigate the functional performance of the PDS detection plane and collimator, and of anticoincidence (AC) lateral shields system. The lateral shields are of key relevance because they will also be used as Gamma-Ray Burst Monitor (GRBM). The GRBM expected performance has already been investigated and results are reported [4, 5].

2. – Detector description

A summary of the main features of the PDS as expected on the basis of its design is given in table I.

The PDS detector is made of three main components: the phoswich assembly, the collimator assembly, the shield assembly. The phoswich plus collimator assemblies make the Core Assembly (CA).

Figure 1 shows a photo of the flight model of the phoswich assembly. It consists of an array of four NaI(Tl)/CsI(Na) phoswich scintillation detectors each viewed by a photomultiplier tube (PMT) EMI D-611. The total detection area is 795 cm^2. The CsI(Na) scintillator, which is optically coupled with the NaI(Tl) detector, acts as an active shield, reducing the environmental radiation impinging on the primary NaI(Tl) detector and rejecting events that leave only a part of their energy in the primary NaI(Tl) detector. CsI(Na) acts also as a light guide.

At the center of the detection plane, there is a fixed calibration source (FCS). It consists of a ^{241}Am radioactive source distributed within a plastic scintillator (BC-400) viewed from a PMT (Hamamatsu R 1635). Part of the 60 keV X-rays emitted by this source impinges on the 4 phoswich detectors. These events are tagged thanks to the α particles simultaneously emitted with them and detected by the plastic scintillator. The FCS permits

TABLE I. – *Main design features of the* PDS *instrument.*

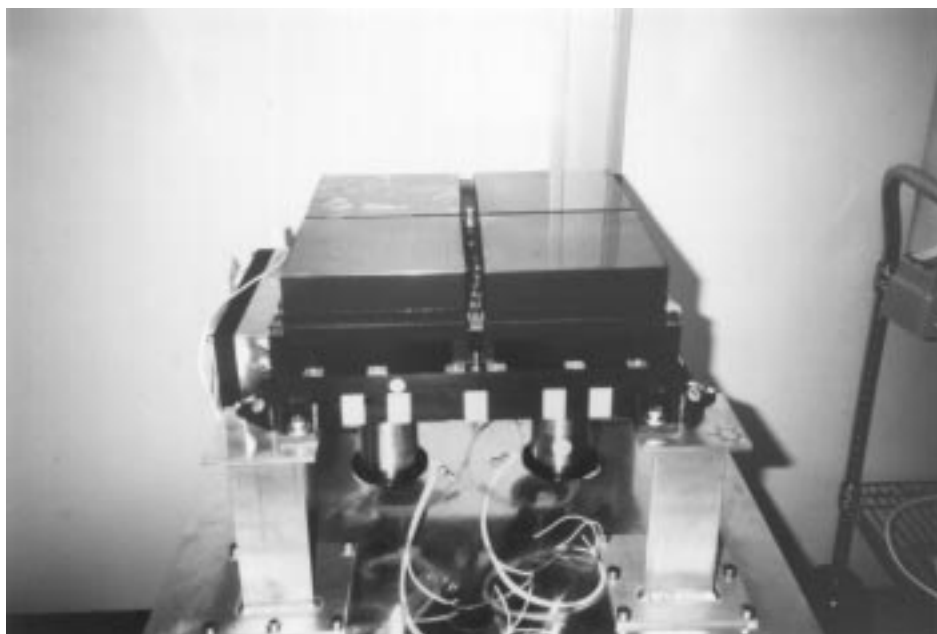| Parameter	Value
Energy range	15–300 keV
Total detector area	795 cm^2
Energy resolution at 60 keV	$\leq 17\%$
Time resolution	20 μs
Field of view (FWHM)	$1.4°$ hexagonal
Gain control accuracy	0.25%
In-flight calibration accuracy	0.1%
Minimum channel width of energy spectra	0.3 keV
Telemetry rate:	
a) normal	~ 10 Kbps
b) maximum	50 Kbps
Temperature operative range	10–30 $°$C

Fig. 1. – Photo of the PDS Crystal Assembly. The Fixed Calibration Source (FCS) is also apparent.

a continuous automatic gain control of each phoswich unit plus electronic chain. However, it is not suitable to be used as an absolute calibrator, since the FCS photons impinge only on a small part of the phoswich detector surfaces. Due to a disuniformity in the phoswich gain across the surface (see below), a bias in the detector gain can derive.

The collimator assembly consists of two X-ray collimators made of tantalum tubes with hexagonal section. Within each tube a Tin + Copper layer 4 cm from the its bottom is used to attenuate the X-ray fluorescence of the collimator materials. The collimators are positioned above the phoswich detection units. The collimators limit the detector field of view to $1.4°$ full width at half-maximum (FWHM). Each of the two collimators can be independently rocked back and forth with respect to the neutral position to allow the simultaneous measurement of the background level and source flux.

Figure 2 shows the Shield Assembly (SA). It includes three main components: the lateral shield assembly, the top shield assembly and the movable calibration system (MCS). The lateral shield assembly consists of four independent slabs of CsI(Na) scintillators of 10 mm thickness that surround the detection plane and the collimator assembly. Each slab is viewed from two PMTs (Hamamatsu R-2238). A pulser made of an ^{241}Am source encapsulated in a small NaI(Tl) scintillator is inserted in each slab to produce a gamma-equivalent energy within the range from 350 to 450 keV.

The top shield assembly consists of a 1 mm thick plastic scintillator (BC-400) viewed from 4 PMTs (Hamamatsu R-1840). It is positioned above the collimator assembly and covers the X-ray entrance aperture.

The lateral shield and the top shield assemblies form an efficient anticoincidence shield to unwanted X-ray photons and/or charged particles.

The MCS is an in-flight calibrator made of a radioactive source of ^{57}Co (main lines at 14 and 122 keV) distributed along a wire, and contained in a cylinder of lead that shields the radioactive source but a small aperture toward the crystal assembly. The MCS peri-

Fig. 2. – Photo of the PDS Shield Assembly.

odically crosses the FOV of the telescope with constant speed, allowing the monitoring of the absolute gain of the instrument.

3. – Instrumentation for performance tests

The phoswich assembly was tested using the electronic chain shown in fig. 3. It is a standard NIM spectroscopy chain inclusive of pulse shape analysis. The signals from a phoswich PMT are sent to a charge preamplifier and then to a delay line amplifier with a shaping time of 2 μs. The signals from the amplifier are sent to both a delay amplifier and a constant fraction pulse shape analyzer (PSA, ORTEC 552). The pulses that are qualified as good events by the PSA are analog-to-digital converted (ADC). The pulse height spectrum is acquired by a Personal Computer for on-line display, further analysis and archiving.

A light pulser encapsulated in each phoswich crystal allows to simulate a prefixed gamma-equivalent energy (GEE) lost in the phoswich. Also an electronic pulser (Canberra 1407) is used to monitor the gain of the electronic chain during the measurements.

The electronic chain used to test the shield assembly was similar to the previous one. In this case the PSA was used to separate the signals from the CsI(Na) slab from those coming from the pulser.

The angular response of the collimator assembly was only tested with a uniform optical beam. The scheme of the apparatus is shown in fig. 4. The source of the optical beam is a He/Ne stabilized laser (LASER). The optical beam, before impinging the X-ray collimator, is expanded by an optical system that includes the two lenses L_1 and L_2, and the pin-hole PH. The zeroth-order diffracted separation system is composed by the two lenses L_3 and L_4, while the detection-acquisition electronics is composed by an IBM-PS2 computer, a scanner, a multimeter, and the photodiodes RIV 1 and RIV 2.
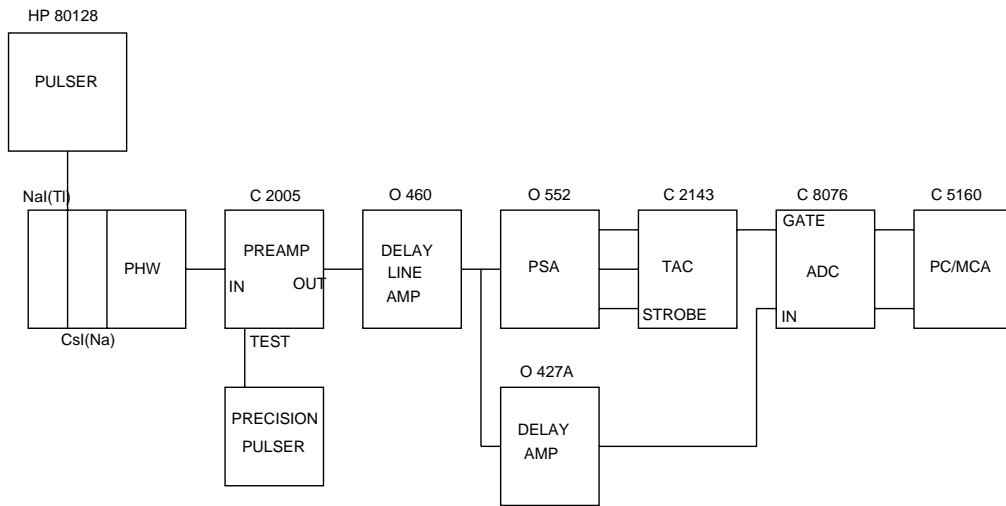
Fig. 3. – Block diagram of the standard electric chain used to test phoswich and shield assembly detectors.
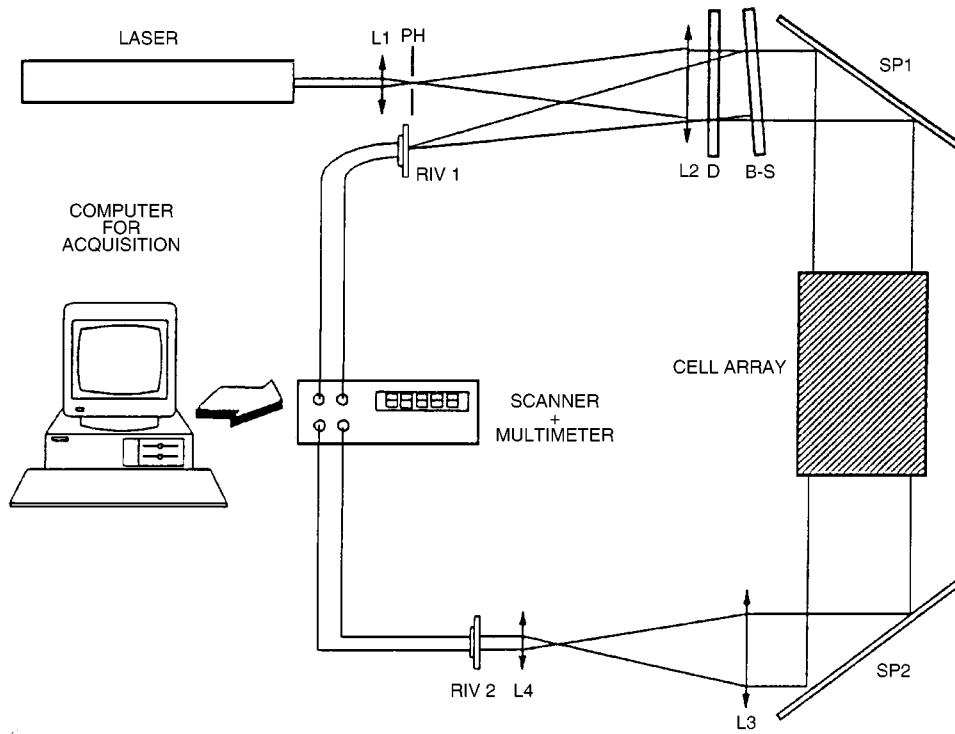

Fig. 4. – Block diagram of the instrumentation used to derive the optical response of the PDS collimators.

The components D, B-S, SP$_1$ and SP$_2$ are, respectively: a circular diaphragm that reduces the beam diameter at the chosen value, a beam-splitter that reflects a part of the probe beam in the direction of the photodiode RIV 1 to create a reference signal, and a couple of folding mirrors with optical surface tolerance less than $\lambda/2$ that fold the beam without introducing significant wavefront distortions.

4. – Performance tests

4'1. *Phoswich units.* –

4'1.1. Tests at nominal operating voltage. Each phoswich was operated at a high voltage such to produce a PMT gain of 1×10^5 (nominal voltage). The
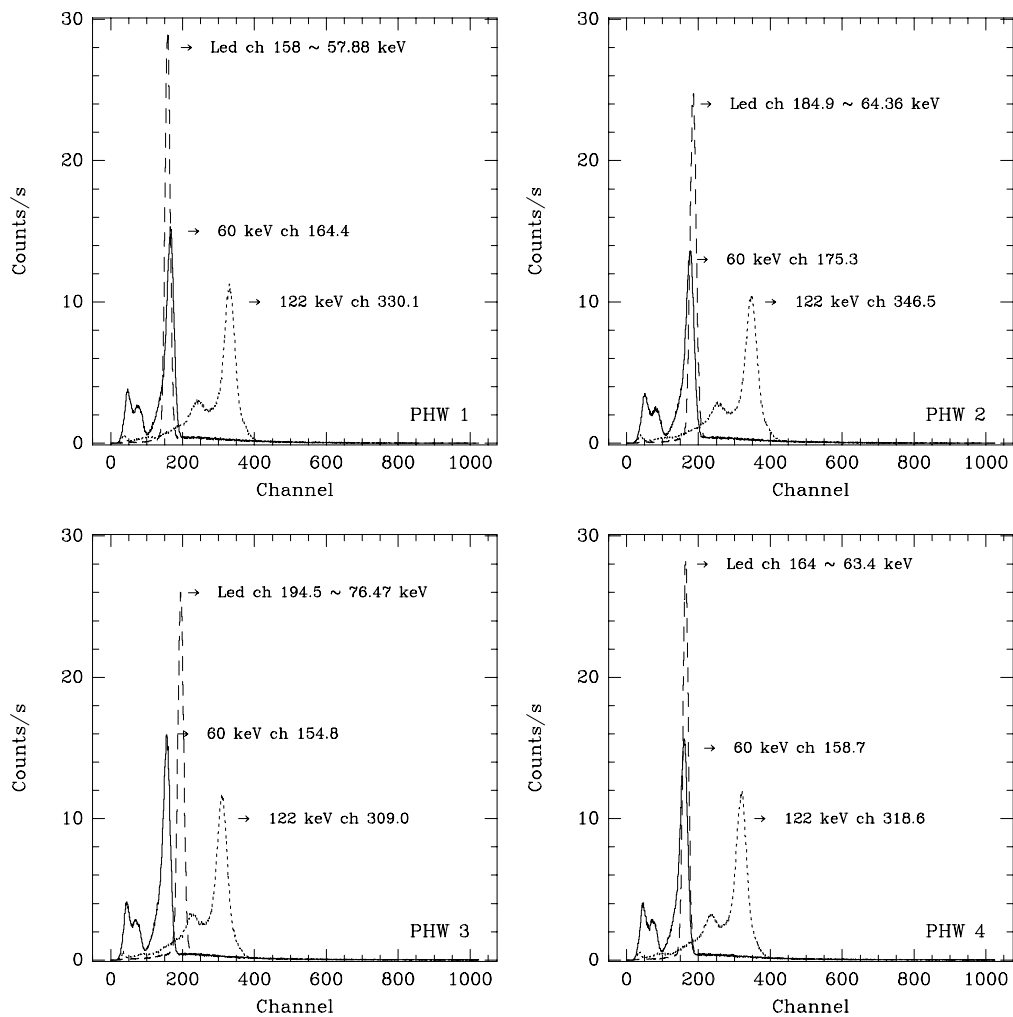

Fig. 5. – Superposition of the energy spectra of ^{241}Am and ^{57}Co as detected by each of the PDS phoswich detectors. The line due to a light pulser (Led) is also shown.
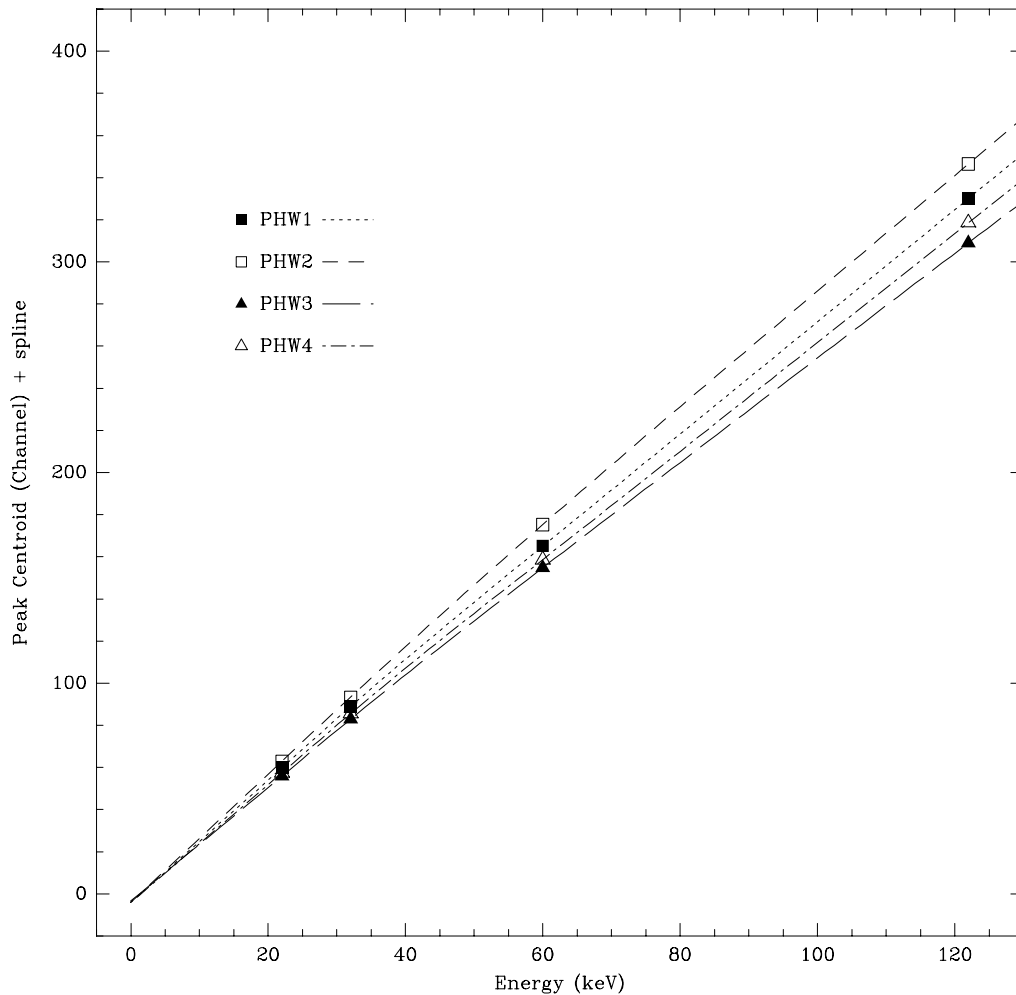
Fig. 6. – Energy-ADC channel relationship for each of the PDS phoswich detectors derived from measurements with radioactive sources (see text).

performance of the phoswiches was evaluated through the use of the following radioactive sources: ^{241}Am (line used 60 keV), ^{57}Co (14 keV and 122 keV), ^{109}Cd (22 keV and 88 keV), ^{137}Cs (32 keV), ^{133}Ba (356 keV). In order to simulate an almost uniform beam impinging on the phoswiches, the sources were positioned, but ^{133}Ba, at 61 cm far from the detectors. The latter source was positioned at a distance of about 150 cm from the detectors.

The superimposed energy spectra of ^{241}Am and ^{57}Co as detected by each phoswich unit are shown in fig. 5. The line due to the light pulser (LED) is also shown. By fitting each known energy line with a Gaussian function, we derived the relevant parameters of the line, *i.e.* intensity (I), centroid channel (C) and full width at half-maximum (FWHM).

The derived energy/MCA channel relationship is shown in fig. 6, obtained by fitting the data with splines. It is apparent a good linearity of the detectors in the operative
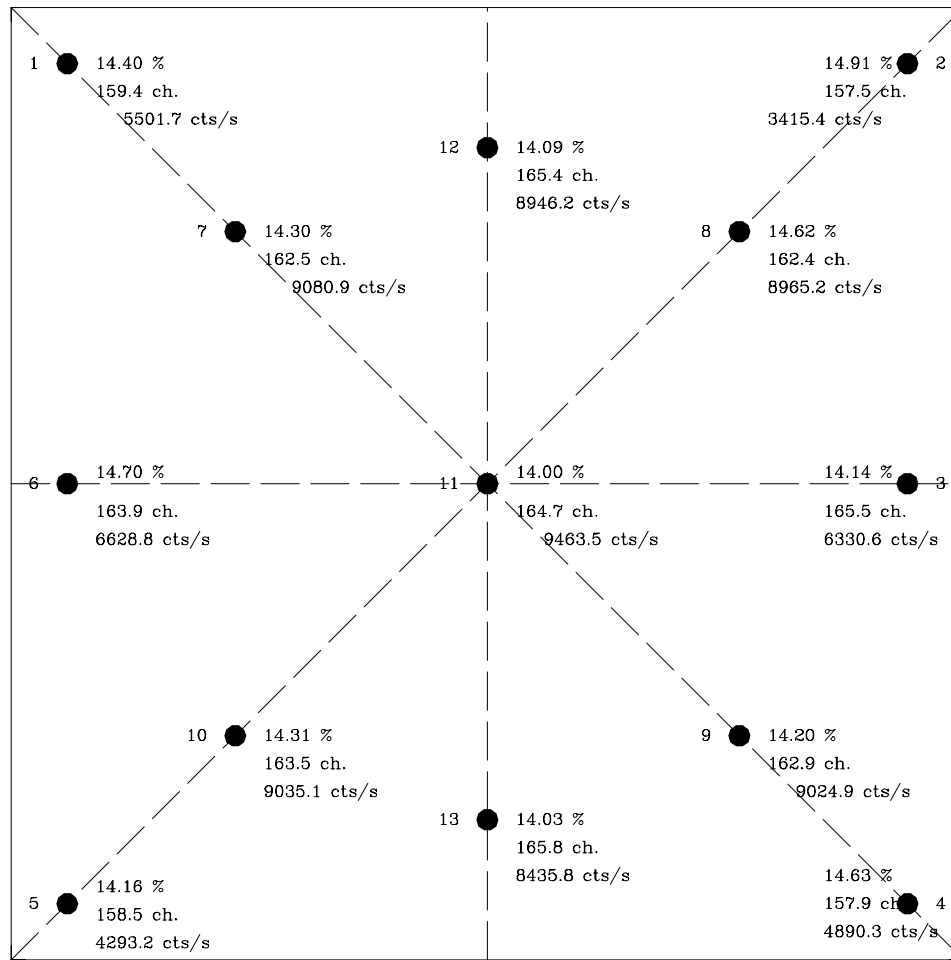
1 ● 14.40 %
159.4 ch.
5501.7 cts/s

14.91 % ● 2
157.5 ch.
3415.4 cts/s

12 ● 14.09 %
165.4 ch.
8946.2 cts/s

7 ● 14.30 %
162.5 ch.
9080.9 cts/s

8 ● 14.62 %
162.4 ch.
8965.2 cts/s

6 ● 14.70 %
163.9 ch.
6628.8 cts/s

11 ● 14.00 %
164.7 ch.
9463.5 cts/s

14.14 % ● 3
165.5 ch.
6330.6 cts/s

10 ● 14.31 %
163.5 ch.
9035.1 cts/s

9 ● 14.20 %
162.9 ch.
9024.9 cts/s

13 ● 14.03 %
165.8 ch.
8435.8 cts/s

5 ● 14.16 %
158.5 ch.
4293.2 cts/s

14.63 % ● 4
157.9 ch.
4890.3 cts/s

Fig. 7. – Result of a mapping of phoswich unit No. 1 with a radioactive source of ^{241}Am. For each point ADC channel of the 60 keV line centroid, line intensity and energy resolution are shown.

range of the PDS. Actually deviations from linearity in NaI(Tl) scintillators are expected in the 20–60 keV energy range (see, *e.g.*, [6]) but they could not be investigated with the available radioactive sources. We intend to derive the exact behaviour of the detectors in the 15–150 keV energy range, using flight spare model (FSM) of the phoswich assembly. The latter is expected to show the same behaviour, since the material used was extracted from the same NaI(Tl) ingot.

The energy resolution of each phoswich for each line energy E, defined as $R(E) \sim$ FWHM$(E)/C(E)$, was also evaluated. For a uniform illumination of the crystals, at 60 keV it ranges from 14.7% to 14.9%, depending on the detection unit, with negligible statistical error. This figure is better than that expected in the instrument design (see table I).

Also a study of the disuniformity of light collection of the phoswich units with the position of the X-ray interactions on the crystal was performed. For that, a collimated source of ^{241}Am was moved in 13 different positions over each crystal and energy spectra for each position were acquired. The results for the phoswich No. 1 are shown in fig. 7, where
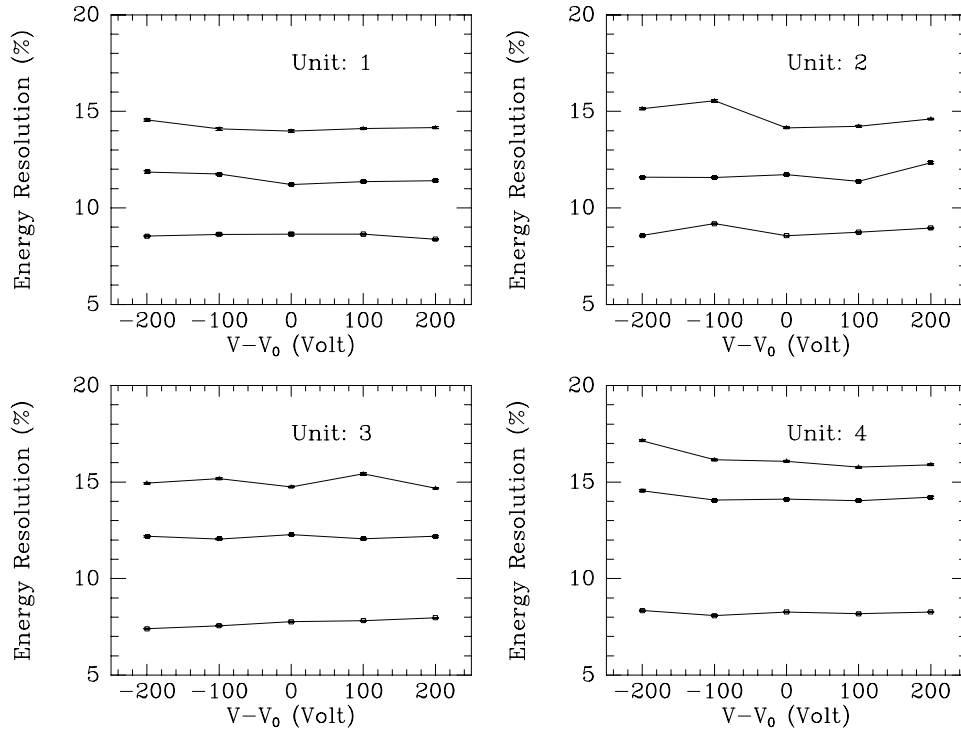
Fig. 8. – Energy resolution of the phoswich NaI detectors as a function of the difference between the PMT high-voltage supply and the nominal high voltage of each PMT. From bottom to top: Led (open square), 122 keV (solid square), 60 KeV (solid triangle).

centroid peak and energy resolution at the different positions are shown. As can be seen, the maximum gain decreases moving from the crystal centre to one of the edges by about 4.1%.

4'1.2. Tests at different high voltages. In order to determine the interval of high-voltage supply within which the phoswiches can be operated, the detector gain and energy resolution was determined at different PMT high voltages. We performed the tests in a range of ± 200 V around the nominal HV. Figure 8 shows the dependence of the energy resolution on HV for each of the phoswich units. As can be seen, in the HV range tested, the energy resolution at 60 keV results to be constant within statistical uncertainties.

4'1.3. Thermal-vacuum tests. Each phoswich was individually placed in a vacuum chamber with a ^{241}Am radioactive source at a distance of about 20 cm. At the same temperature in which the previous tests were performed, no degradation of the performance was observed while the detectors were operated in vacuum conditions, nor during the passage from atmospheric pressure to vacuum.

The relative light output of each phoswich with temperature was also tested in vacuum conditions. Figure 9 shows the dependence of the peak centroid of the 60 keV line as a function of crystal temperature. A general decrease of the gain with temperature is apparent. The maximum fractional variation (9%) with respect to the gain at 0 °C was
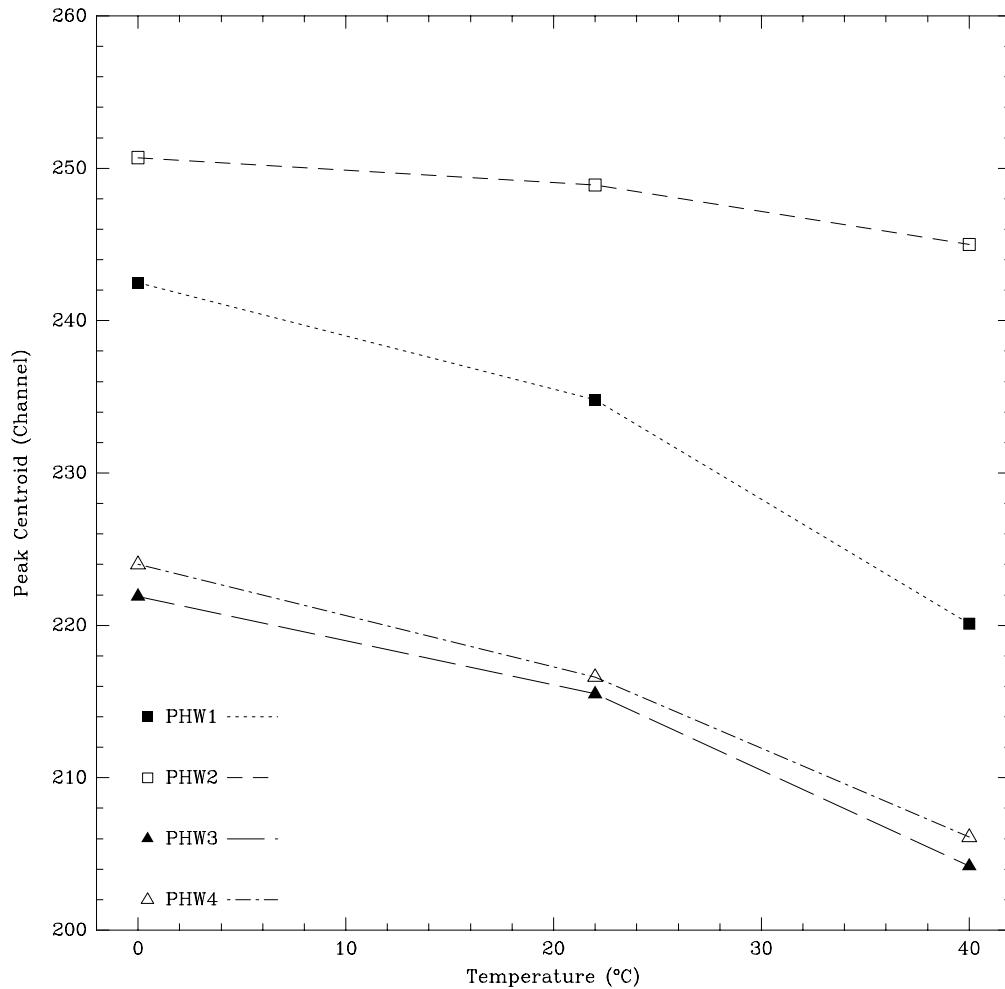
Fig. 9. – Gain of each phoswich NaI detector at 60 keV as a function of detector temperature. For this test the crystal assembly was inside a vacuum chamber.

observed for phoswich No. 1. This trend is due to the combined dependence of PMT quantum efficiency and NaI(Tl) light yield on temperature.

4˙2. *Lateral shields assembly.* – Given the additional function of the lateral shields as GRBM, deeper performance tests than those required as AC shield were performed. They included tests before the single detection slabs were integrated into the shields assembly and tests after the integration. On the integrated shields assembly, successful thermal-vacuum tests and vibration tests were performed. We report here only on some relevant tests.

4˙2.1. A v e r a g e   p r o p e r t i e s   o f   e a c h   s l a b. Gain and energy resolution of each detection slab, before being integrated into shield assembly, was measured by using radioactive sources of ^{109}Cd, ^{241}Am, ^{57}Co, ^{22}Na and ^{137}Cs positioned at a distance of 100
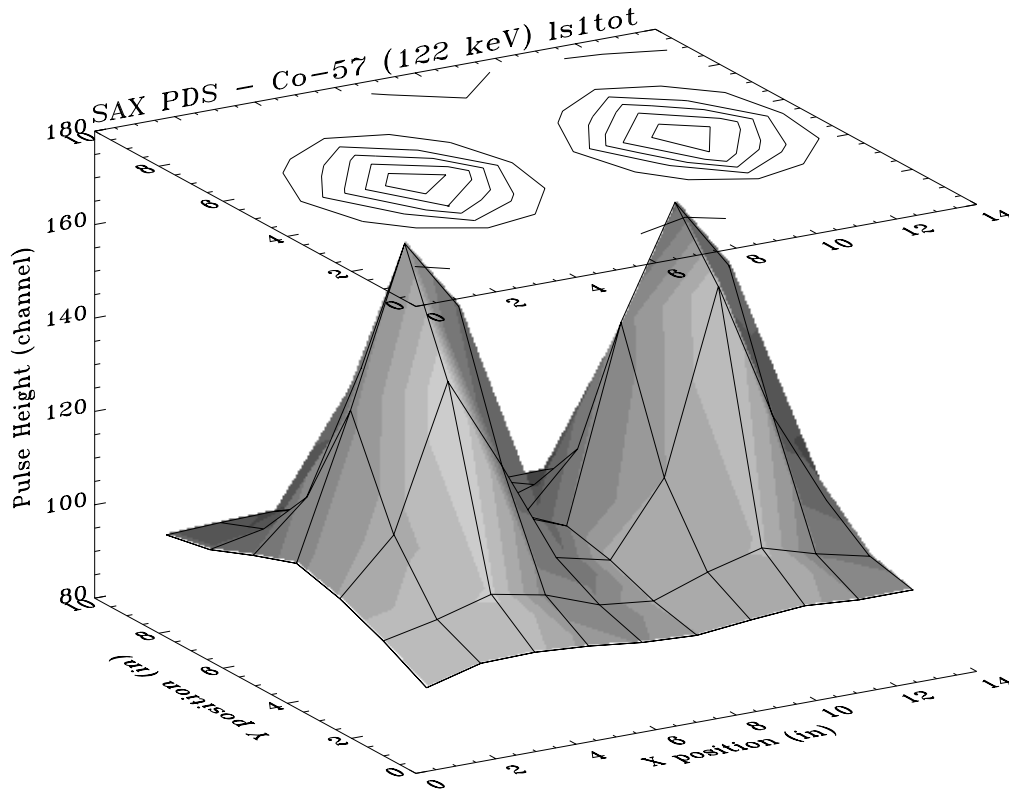
Fig. 10. – Mapping of the gain of the lateral shield No. 1 at 122 keV. Maximum gain corresponds to the PMTs centre position.

cm. The detectors were operated at a nominal high voltage to produce a PMT gain of 1×10^5. The PMT anodes were summed and the resulting signal was sent to the same electronic chain used to test phoswich detectors (see sect. **3**). The shaping time of the delay line amplifier was set to 2 μs. The linearity of the detectors up to 662 keV resulted to be very good and the mean energy resolution was 43% at 22 keV, 33% at 60 keV and 13.5% at 662 keV. Statistical uncertainties were negligible. The dependence of the energy resolution with energy was consistent with $R(E) \propto 1/\sqrt{E}$.

The gamma-equivalent energy (GEE) of the light pulser was determined too. It resulted to be dependent on the detector and ranging from 350 keV to about 450 keV.

Gain and energy resolution were also evaluated when the HV supply was varied in the range ± 200 Volts with respect to the nominal one. Energy resolution remained constant in this HV range.

4˙2.2. U n i f o r m i t y   t e s t s   o f   e a c h   s l a b. The response of each detection slab with the position of photon interaction in the crystal was also measured. For that a collimated source of ^{57}Co, that produced a circular spot with a diameter of about 10 mm in the crystal was used. The maximum gain was found when the source was positioned directly underneath the PMTs, while the minimum gain was measured in correspondence of the slab edges. The disuniformity, defined as (*maximum centroid channel – minimum cen-*
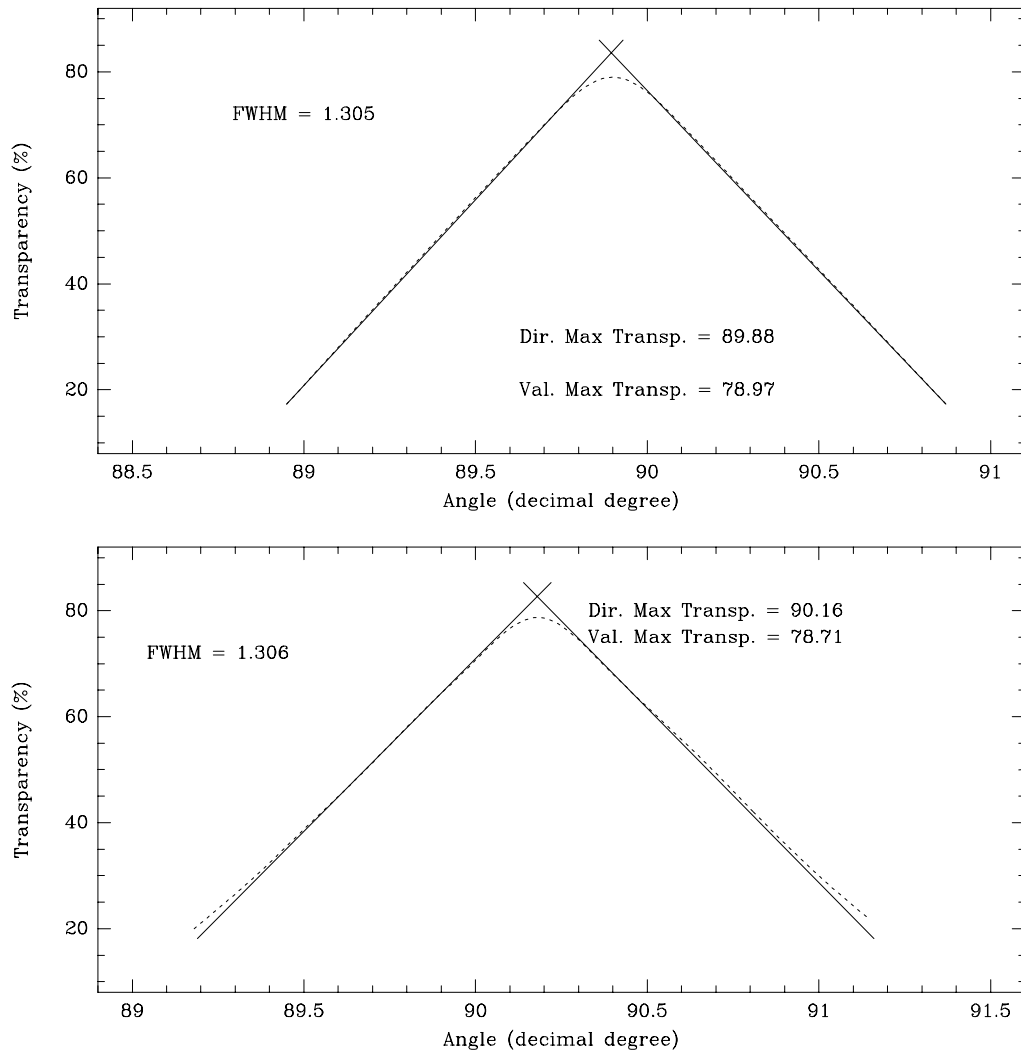
Fig. 11. – Angular response of one of 4 sub-collimators with optical light along two perpendicular directions. The on-axis average transparency is 80%.

troid channel)/mean centroid channel, resulted to range from 68% to 77%, depending on the detection slab. The gain disuniformity map is shown in fig. 10 for one of the detectors.

4`3. *Collimator assembly*. – Each bank of collimators was tested with laser light with the experimental set-up shown in fig. 4 in order to study the geometry of all collimator cells and thus the angular response of the collimators. The results can be extrapolated to the X-ray band in the assumption of a completely absorbing material. The angular response in the X-ray band will be also measured on-ground using the flight spare model of the collimator assembly and with celestial sources during the performance verification

phase soon after the SAX launch.

The average angular response along one of the axes crossing the sides of the hexagonal cells for one of the collimator banks is shown in fig. 11.

5. – Conclusions

Most of the functional tests performed on the PDS detector resulted in agreement with the design expectations. The energy resolution of the phoswich detectors is better than expected. All this gives the needed confidence that the instrument will achieve the expected scientific capabilities.

* * *

REFERENCES

[1] SCARSI L., *Astron. Astrophys. Suppl.*, **97** (1993) 371.
[2] FRONTERA F., DAL FIUME D., PAMINI M., POULSEN J. M., BASILI A., FRANCESCHINI T., LANDINI G., SILVESTRI S., COSTA E., CARDINI D., EMANUELE A. and RUBINI A., *Adv. Space Res.*, **8** (1991) 281.
[3] FRONTERA F., DAL FIUME D., PAMINI M., POULSEN J. M., ZHANG C. M., BASILI A., FRANCESCHINI T., LANDINI G., SILVESTRI S., COSTA E., CARDINI D., EMANUELE A., and RUBINI A., *Nuovo Cimento C*, **15** (1992) 867.
[4] PAMINI M., NATALUCCI L., DAL FIUME D., FRONTERA F., COSTA E. and SALVATI M., *Nuovo Cimento C*, **13** (1990) 337.
[5] ALBERGHINI F., DAL FIUME D., FRONTERA F. and PIZZICHINI G., *AIP Conf. Proc.*, **307** (1994) 638.
[6] KNOLL G. E., *Radiation Detection and Measurement* (John Wiley & Sons, New York) 1989.